



Nano-mechanical properties of starch and gluten biopolymers from atomic force microscopy

Emna Chichti, Matthieu George, Jean-Yves Delenne, Farhang Radjai, Valérie Lullien-Pellerin

► To cite this version:

Emna Chichti, Matthieu George, Jean-Yves Delenne, Farhang Radjai, Valérie Lullien-Pellerin. Nano-mechanical properties of starch and gluten biopolymers from atomic force microscopy. European Polymer Journal, 2013, 49 (12), pp.3788-3795. 10.1016/j.eurpolymj.2013.08.024 . hal-02648905

HAL Id: hal-02648905

<https://hal.inrae.fr/hal-02648905>

Submitted on 30 Jul 2024

HAL is a multi-disciplinary open access archive for the deposit and dissemination of scientific research documents, whether they are published or not. The documents may come from teaching and research institutions in France or abroad, or from public or private research centers.

L'archive ouverte pluridisciplinaire **HAL**, est destinée au dépôt et à la diffusion de documents scientifiques de niveau recherche, publiés ou non, émanant des établissements d'enseignement et de recherche français ou étrangers, des laboratoires publics ou privés.

Manuscript Number: EUROPOL-D-13-00611R1

Title: Nano-mechanical properties of starch and gluten biopolymers from Atomic Force Microscopy

Article Type: Research Paper

Section/Category: Nanotechnology

Keywords: AFM; Biopolymer; Hardness; Friction; Scratch test

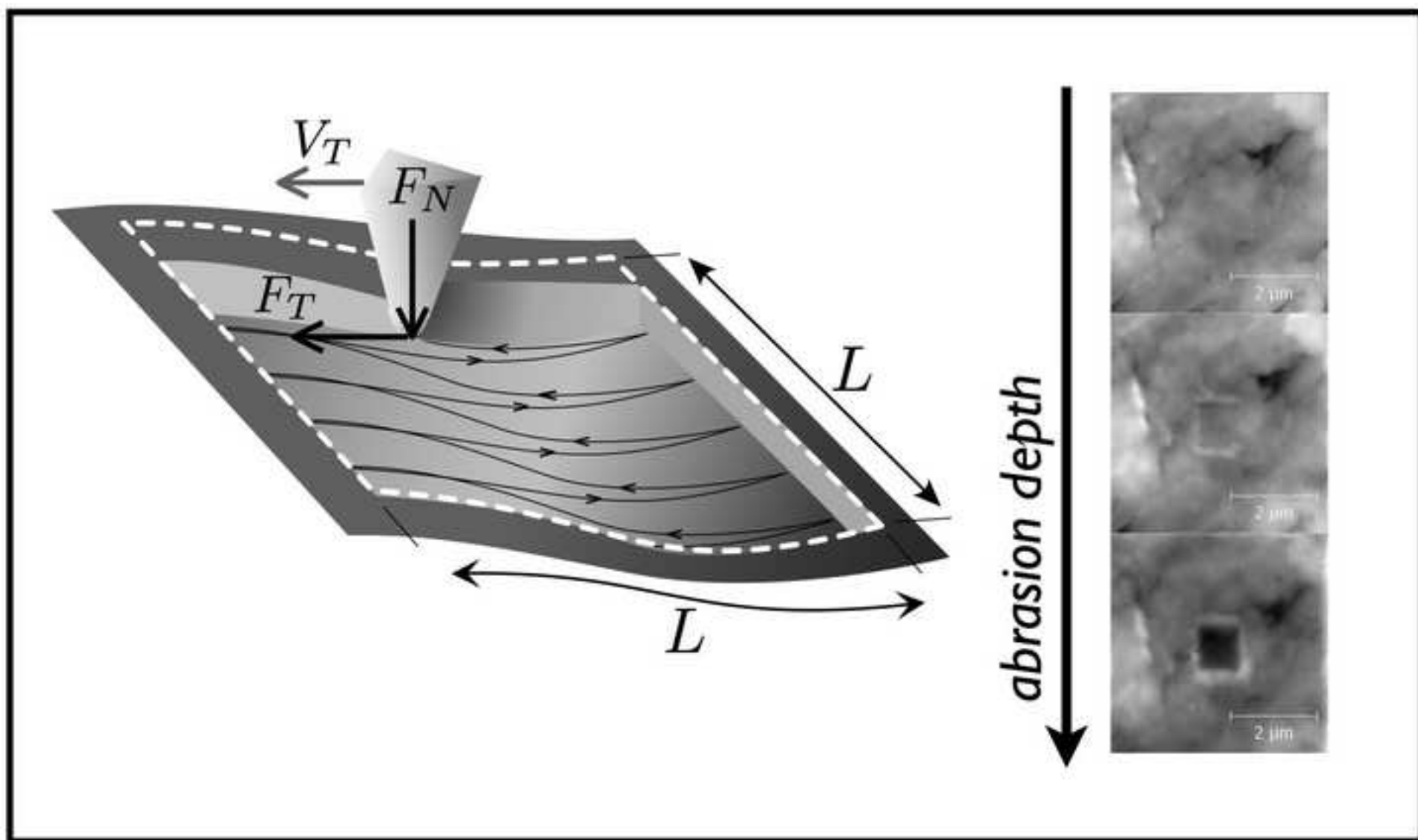
Corresponding Author: Dr. Valérie Lullien-Pellerin,

Corresponding Author's Institution:

First Author: Emna Chichti

Order of Authors: Emna Chichti; Mathieu George; Jean-Yves Delenne; Fahrang Radjai; Valérie Lullien-Pellerin

Abstract: An original method based on atomic force microscopy (AFM) in contact mode was developed to abrade progressively the surface of tablets made of starch or gluten polymers isolated from wheat. The volume of the material removed by the tip was estimated from the analysis of successive topographic images of the surface, and the shear force was measured by keeping a constant normal force. Our data together with a simple tribological model provide clear evidence for a higher hardness and shear strength of starch compared to gluten. Gluten appears to have mechanical properties close to soft materials, such as talc, whereas starch displays higher hardness close to calcite. Our results are in a better agreement with structural properties of gluten (complex protein network) and starch (granular and semi-crystalline structure) than earlier studies by micro-indentation. This work shows that the AFM scratching method is relevant for the characterization of any polymer surface, in particular in application to materials made of different polymers at the nano-scale.



Highlights

- Scratching with AFM tip was used to screen polymer resistance
- A tribological model was developed to determine polymer hardness
- The methodology is used to reveal hardness contrasts in biomaterials at nanoscale
- Wheat starch was found to display higher hardness and shear strength than gluten

Nano-mechanical properties of starch and gluten biopolymers from Atomic Force Microscopy

Emna Chichti^{a,c}, Matthieu George^b, Jean-Yves Delenne^a, Farhang Radjai^c,
Valérie Lullien-Pellerin^{a,1},

^aINRA, UMR 1208, Ingénierie des Agropolymères et Technologies Emergentes, F-34060
Montpellier Cedex 01, France

^bLaboratoire Charles Coulomb, UMR 5221, CNRS-UM2, Place Eugène Bataillon,
F-34095 Montpellier Cedex, France

^cLaboratoire de Mécanique et Génie Civil, UMR 5508, CNRS-UM2, Place Eugène
Bataillon, F-34095 Montpellier, France

Abstract

An original method based on atomic force microscopy (AFM) in contact mode was developed to abrade progressively the surface of tablets made of starch or gluten polymers isolated from wheat. The volume of the material removed by the tip was estimated from the analysis of successive topographic images of the surface, and the shear force was measured by keeping a constant normal force. Our data together with a simple tribological model provide clear evidence for a higher hardness and shear strength of starch compared to gluten. Gluten appears to have mechanical properties close to soft materials, such as talc, whereas starch displays higher hardness close to calcite. Our results are in a better agreement with structural properties of gluten (complex protein network) and starch (granular and semi-cristalline structure) than earlier studies by micro-indentation. This work shows that the AFM scratching method is relevant for the characterization of any polymer surface, in particular in application to materials made of different polymers at the nano-scale.

Keywords: AFM, Biopolymer, Hardness, Friction, Scratch test

¹Corresponding author. Tel: +33 4 99 61 31 05
Email address: lullien@supagro.inra.fr (V. Lullien-Pellerin)

1. Introduction

Wheat is a major cereal crop for both food and non-food industries. The starchy endosperm, which is the main constituent of wheat grains (80-85%), contains two important biopolymers, which display unique rheological properties [1, 2, 3] : starch (80-90% of dry mass) in the form of granules which are embedded in a gluten matrix, mainly made of the storage proteins [4].

Food products, such as bread, biscuits or pasta, are made of flour and semolina which are obtained by the isolation of wheat grain endosperm and its reduction by dry fractionation in successive steps of grinding and sieving. In turn, further processing of flour and semolina can be undertaken to isolate starch and gluten biopolymers which are used in food industry, e.g. as additives to adjust food rheology, and in non-food applications to replace petroleum-based packaging materials [5, 6, 7], coating agents in paper industries [8, 9] or adhesives [10, 11] due to their renewability, physical properties and biodegradability. Purified starch is also employed as a starting material in petrochemical processes [9].

Therefore for a better control of the endosperm product quality, it is necessary to better characterize the fractionation behavior of the wheat endosperm which is clearly related to its structure and mechanical properties. The endosperm structure could be related to a granular cemented material and a numerical model was built in order to identify key factors, which could play a role in its mechanical behaviour [12, 13]. The model was based on actual knowledge of the endosperm structure and organization and took into account the described mechanical properties of starch and protein that were reported to be identical based on micro-indentation assays [14, 15]. The model showed that the fracture propagates differently depending on both the protein content and the starch/protein matrix adhesion. However, lack of information about the polymer mechanical properties at a nano-scale constitutes a major limitation for the modeling construction.

In this paper, we investigate the mechanical properties of isolated unmodified wheat starch and gluten with an original AFM nanoscratch approach. Since its invention [16], AFM has proved to be a powerful tool for topographical imaging at the nanoscale and with minimal sample preparation, of various biomolecules such as nucleic acids, proteins, polysaccharides, but also for the measurement of their mechanical properties [17, 18]. AFM has already been employed to characterize the surface topography of wheat starch and to compare its structure to starch isolated from other plant resources

[19, 20]. Similar topographic studies were also reported for some of the storage proteins forming the gluten network. Gliadins (α, ω) interactions in different solvent conditions [21], as well as non-covalent interactions between glutenins of high molecular weight [22], have been investigated by means of AFM but with slight modifications of the molecules by either immobilisation or reduction and alkylation. Wheat endosperm was also tentatively observed using AFM to compare the endosperm structure in wheat grains differing by their hardness, but the method was unable to discern between starch and gluten polymers even if some differences in surface morphology were observed depending on the wheat genetic origin [23].

Indentation or scratching assays are generally used to probe the mechanical properties of different polymers from the nano to micro-scale [24, 25]. Recently, Kurland et al. [26] reviewed how AFM could be used for nano-indentation under native conditions to access the Young modulus of globular, fibrous and filamentous proteins. New developments have also been reported on the use of an AFM tip to abrade a target sample surface for the measurement of cohesive energy in a biological material [27]. Similar scratching tests on polymers by means of a nanoindenter were used for friction analysis [28] and determination of shear strength [29]. But, to our best knowledge, AFM has never been used as a tool to characterize the mechanical properties, i.e. hardness and shear stress of such biopolymers as starch and gluten. In the following, we first present our materials and AFM nanoscratch method. The data will then be analyzed for starch and gluten samples and used to determine their hardness and apparent friction coefficients. A simple tribological model will be used to approach the shear strength of both polymers. Finally, we conclude with the most salient findings and perspectives of this work.

2. Experimental

2.1. Materials

All commercial products, wheat starch (Fluka N°85649, $\leq 0.5\%$ ash, 10.5% water content) and gluten biopolymer (SigmaG5004, 80% protein, 7% fat, 7.5% water content) were purchased from Sigma-Aldrich Co (St-Louis, MO, USA). Starch (98% purity, 11.5% moisture content) and gluten (65% purity, 9.5% moisture content) were also purified from wheat grains displaying distinct hardnesses (hard and soft common wheat cv. Glasgow and Dinor, respectively) using a previously described method [30]. Polymethyl methacrylate (PMMA, Fluka 183350, $T_g = 124^\circ\text{C}$, of average molecular

weight $1.2 \cdot 10^6 \text{ g/mol}$), was used as reference material with known mechanical properties at the nanoscale [31, 25, 32].

2.2. Sample preparation

Several tablets of commercial or extracted starch and gluten powders were prepared with approximate weight of 1 g in a pelletizer (Specac Inc, Smyrna, USA) by applying a pressure of 0.5 MPa during one minute using a laboratory press (Hydraulische Press, Perkin-Elmer, USA). Tablets were stored before analysis under controlled conditions of temperature and humidity (20°C , 30% RH).

2.3. Microscopy

Environmental Scanning Electron Microscopy (ESEM, Fei Quanta 200 FEG, FEI Co, Hillsboro, OR, USA) without sputter coating was used to check the homogeneity and absence of defaults in the samples as well as for imaging AFM tips before and after abrasion.

2.4. AFM assays

AFM assays were performed with a Nanoscope V atomic force microscope (Bruker instruments, Madison, WI, USA), operating in the contact mode under controlled conditions of temperature and humidity (20°C , 30% relative humidity). Commercial Si_3N_4 tips (Bruker) mounted on a rectangular cantilever with stiffness in the range between 1 and 5 N/m were chosen to preserve reasonable measurement sensitivity and to exert sufficiently large forces to abrade the samples. Before each measurement, the normal and tangential forces F_N and F_T , respectively, were calibrated by means of a hard silicon wafer in order to convert the values measured in volts to force units.

The calibration of the normal force was performed through displacement-force plots whereas vertical cantilever stiffness measurements were calibrated by means of the thermal fluctuation method [33]. The friction forces were calibrated using Coulomb's friction law and the value of the friction coefficient for the silicon wafer was fixed ($\mu_{\text{Si-Si}} = 0.1$) according to the studies of Morton et al. [34]. Since AFM calibration was made on hard silicon wafers, the tips are expected to be partially flattened. Several ESEM observations were made, as illustrated in Figure 1a, in order to check the tip geometry before and after calibration. The contacting areas of the tips were characterized through reverse imaging obtained with AFM (Figure 1b) on a calibrating

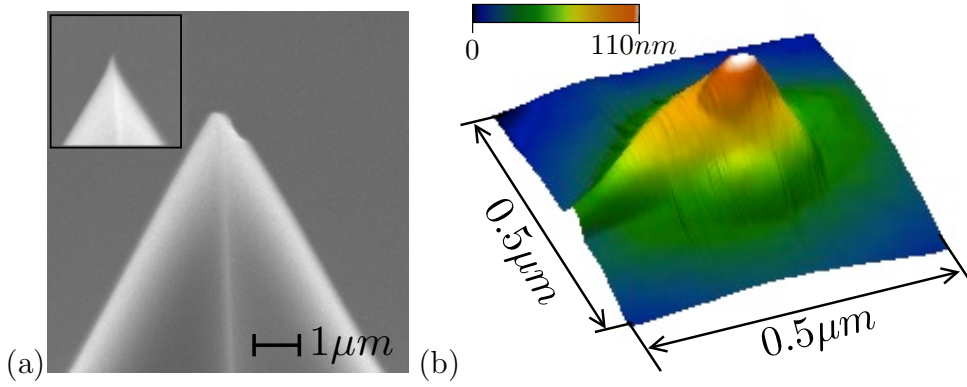


Figure 1: a) ESEM pictures of an AFM tip before (insert) and after calibration; b) Picture in false colors of an AFM tip obtained by mirror imaging with a calibrating grid.

108 grid of equally-spaced sharp points of apex radius $\simeq 10$ nm (TGT01, Mikro-
 109 masch, Inc., Estonia). These measurements clearly showed that the AFM
 110 tip apex can be well fitted after calibration by a sphere from the extremity
 111 to 20 nm high, with an average radius for the set of tips $R = 82 \pm 32$ nm.

112 The AFM assays were conducted, as schematized in Figure 2a, by follow-
 113 ing a procedure inspired by a previously described method [27]. It consists of
 114 successive steps of topographic image acquisition on a large scale and abra-
 115 sive scans on a predefined area by setting the force applied on the AFM
 116 cantilever to the desired value. First, a large ($L \times L > 10 \times 10 \mu m^2$) topo-
 117 graphic image is acquired as the tip scans the sample surface at a low applied
 118 normal force ($F_N = 100nN$) in order to select the appropriate working area
 119 for polymer abrasion, i.e. the center of a starch granule or a homogeneous
 120 gluten area. Then, a smaller topographic image ($5 \times 5 \mu m^2$) at a scan tip
 121 velocity V_T of $10 \mu m/s$ (512×512 pixels) is acquired (step 1) inside the se-
 122 lected area in identical conditions, that will serve as reference image of the
 123 undamaged surface.

124 The abrasion process (step 2) is initiated on the central area ($L \times L = 1 \times 1$
 125 μm^2) with an increase of the applied normal force ($F_N > 200$ nN) and a de-
 126 crease of the scan velocity ($V_T = 2 \mu m/s$, 256×256 pixels). Both the trace
 127 and retrace F_T force maps are acquired (respectively scanning from left side
 128 to right side of the image and from right side to left side) to determine
 129 the average force sustained by the sample in the direction of displacement.
 130 Thereafter, the normal force is decreased back (step 3) to its initial value (100
 131 nN) and a second topographic image ($5 \times 5 \mu m^2$) is recorded at $V_T = 10$

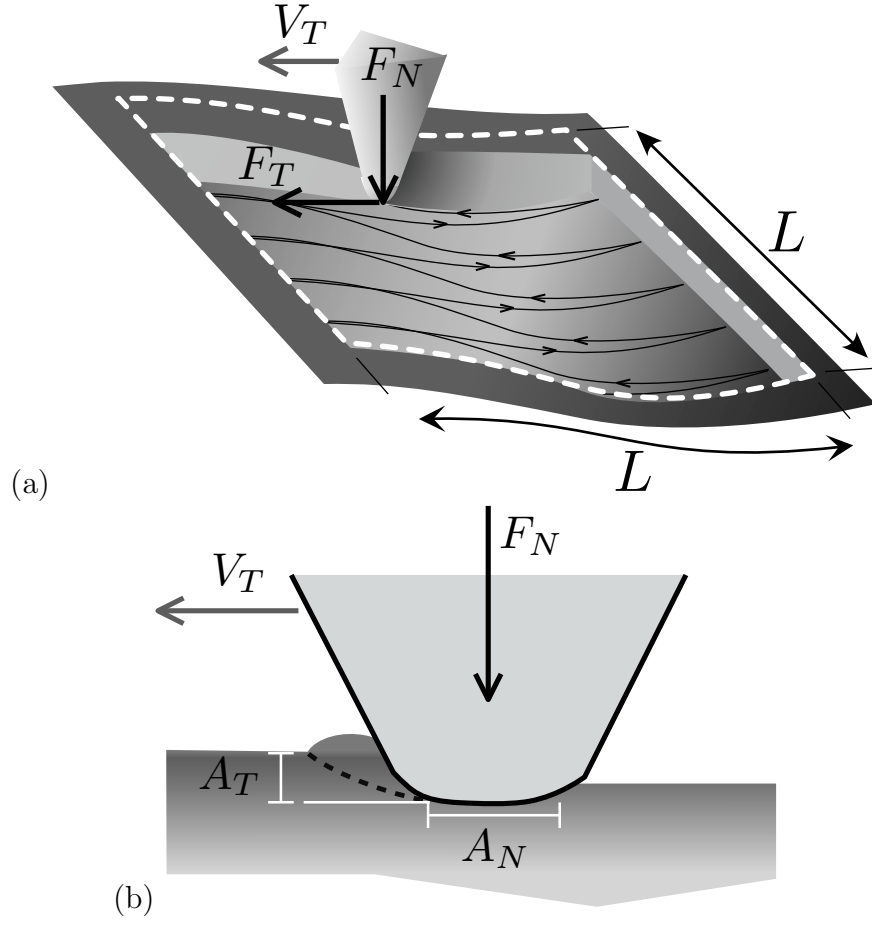


Figure 2: a) Schematic representation of the AFM procedure where F_N is the applied normal force, V_T is scan tip velocity, F_T is friction force and L is the length of the abraded area; b) Schematic description of the abrasion zone where A_N is the projected contact area of the tip on the sample surface and A_T is the projected area in front of the tip in the direction of displacement.

132 $\mu\text{m/s}$ before increasing again the normal force to further abrade the material.
 133 A progressive and controlled abrasion of the polymer sample was ensured by
 134 repeating up to ten times the abrasion step (step 2), interrupted by regular
 135 acquisitions of larger topographic images (step 1) after $N = 1, 4, 7$ and 10
 136 abrasive scans, respectively. This abrasion process was undertaken at least
 137 on ten distinct independent locations for each analysed polymer. The ac-
 138 quired AFM images were visualized and analyzed by means of the software
 139 Gwyddion 2.26 (Department of Nanometrology, Czech Metrology Institute,
 140 Brno, CZ) in order to evaluate the abrasion depth and friction force F_T .

141 2.5. Nano-indentation assays

142 Nano-indentation assays were performed using a diamond Berkovich in-
 143 denter (CSM Instruments, Switzerland, ultranano indentation tester) at an
 144 angle of 141.9° . In the first step, the indenter is placed on the sample surface
 145 by a rough approach at a speed of 2000 nm/min until a contact force (set
 146 to $15\text{ }\mu\text{N}$) is detected. Then, force-displacement curves are acquired under
 147 imposed linear load/unload conditions. For gluten and starch, the maximum
 148 load was set to $50\text{ }\mu\text{N}$, the loading/unloading rate to $25\text{ }\mu\text{N/min}$ and the
 149 pause time between loading and unloading to 20 s . These parameter values
 150 were chosen to be as small as possible in order to avoid the sliding of the
 151 indenter. For bulk PMMA, these parameters were respectively set to $100\text{ }\mu\text{N}$,
 152 $50\text{ }\mu\text{N/min}$ and 30 s for most accurate measurements. The hardness H is
 153 defined as the ratio between the maximum force F_{max} just before unloading
 154 and the projected contact area A_N determined by the tip geometry. The
 155 indentation assays ($n = 20$) were performed by displacements of $10\text{ }\mu\text{m}$.

156 3. Results and Discussion

157 3.1. Evolution of abrasion depths

158 The AFM abrasion tests were performed on tablets prepared by powder
 159 compression to avoid slipping of the starch granule or the protein polymer
 160 along abrasion and also to avoid resin inclusion which may interact with
 161 the analyzed material and influence their mechanical properties. Due to
 162 potential variability of the polymers, reflecting their wheat origin or isolation
 163 method, the tablets were made of either commercially purchased purified
 164 starch and gluten or were extracted in the laboratory from wheat grains of
 165 different genetic background. The abrasion experiments were performed by
 166 a methodology derived from that of Ahimou et al. [27]. The AFM tip was

placed on a homogeneous gluten area or inside a starch granule, as shown in Figure 3 (a-b, a'-b'), and a square of $1 \mu\text{m}^2$ area was scraped. The abrasion area was analyzed by means of $5 \times 5 \mu\text{m}^2$ topographic images taken before and after N abrasion scans. As shown in Figure 3 (c and c'), the abrasion depth in gluten is higher than in starch for a similar applied normal force ($F_N = 480 \text{ nN}$), which indicates a higher resistance to abrasion of starch compared to gluten.

Two different methods were used to measure the volume of the removed material. In fact, the potential lateral drift between successive acquired images and the roughness of the scanned area makes it difficult to determine the total depth of the abraded area after ten abrasive scans. We used the differences between topographic images to measure the depth along the abrasion path. The depth was obtained by averaging only in the central part of the path as the removed material is pushed to the edges. Therefore, the depth reached after N abrasion scans was calculated either as the difference between each topographic image and the initial image (before abrasion) or by cumulating the differences between successive images.

The results of the two methods for depth measurement are presented in Figure 4 for starch and gluten as well as an example of image subtraction. Values obtained by both methods almost coincide. However, the error in the first method (subtraction of each topographic image from the initial image) remains around 10% for the total depth after ten abrasive scans, which is below the 30% error in the second method. A linear increase of the depth was observed at the rates of $11.3 \pm 4 \text{ nm}$ and $1.57 \pm 0.9 \text{ nm}$ per abrasive scan for gluten and starch, respectively. Increasing the applied normal force from $F_N = 480 \text{ nN}$ to $F_N = 2600 \text{ nN}$ led to an increase of the depth after ten abrasive scans to $111 \pm 28 \text{ nm}$ and $15 \pm 4 \text{ nm}$ for gluten and starch, respectively.

The above depth data show clearly that gluten and starch have very different mechanical properties irrespective of their genetic origin. This observation is in strong contrast with earlier studies [14, 15]. It is also important to note that, as the abrasion depth and removed volumes are independent of the scan number, the mechanical behavior in the samples may be considered to be homogeneous.

3.2. Hardness starch and gluten determination

Due to the employed methodology, the abrasion process by the AFM tip can be interpreted as a linear scratching test usually performed to test the

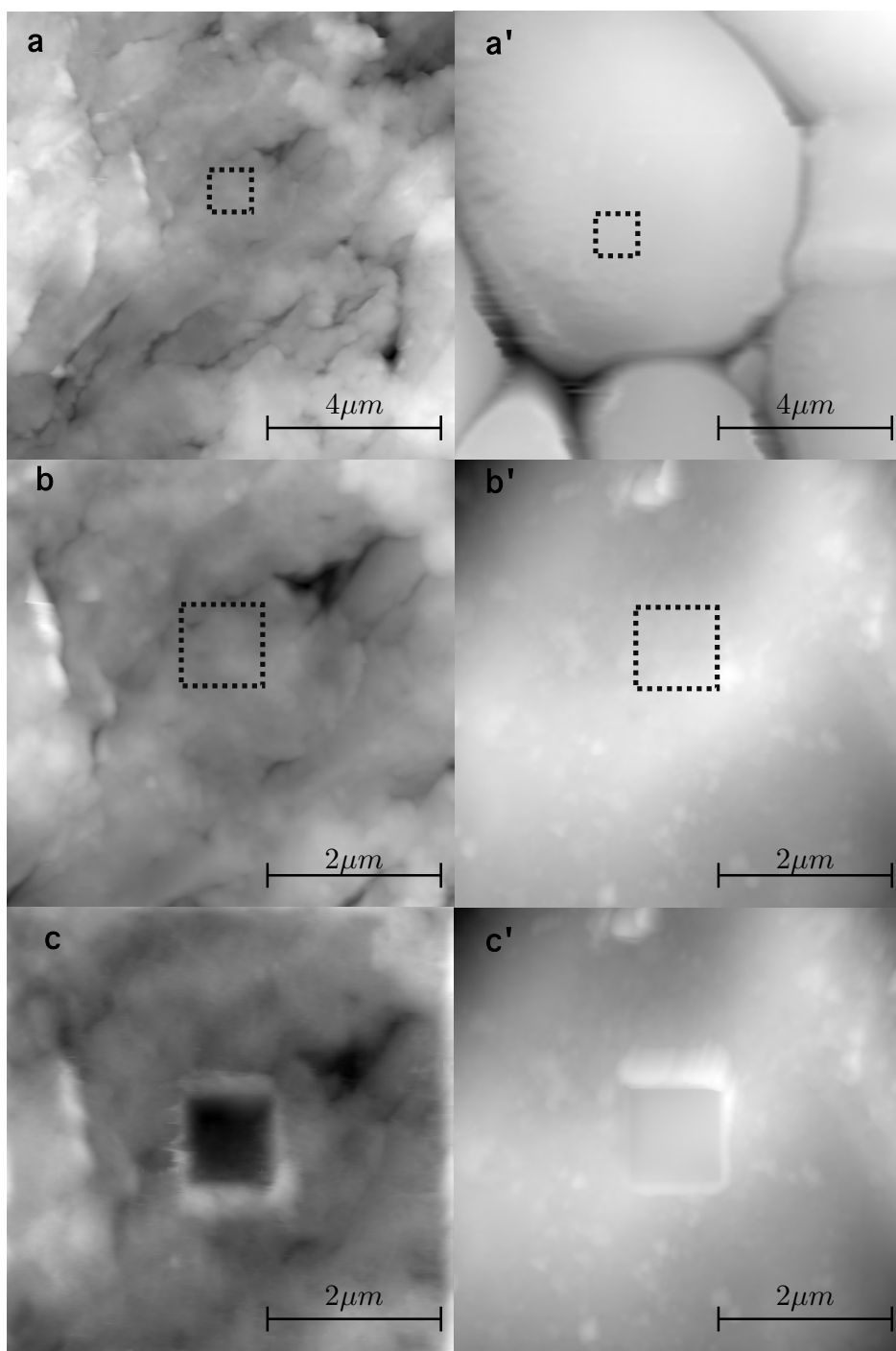


Figure 3: Examples of gluten (a-c) and starch (a'-c') AFM topographic images taken before abrasion at $10 \times 10 \mu\text{m}^2$ (a, a') and $5 \times 5 \mu\text{m}^2$ (b, b') and after 10 abrasive scans (c, c') with an applied normal force of 480 nN. The abrasion zone is marked into the figure with a square

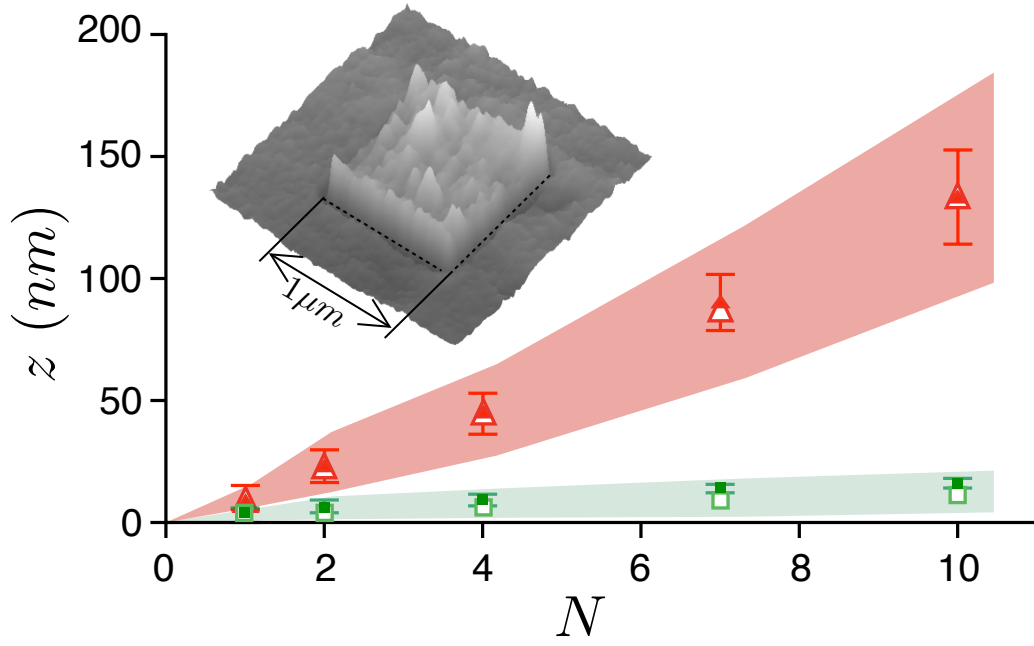


Figure 4: Illustration of different methods of depth (z) measurement as a function of the abrasive scan number (N) in gluten (red triangles) and starch (green squares) subjected to a normal force $F_N = 480$ nN. For each biopolymer, the filled symbols and error bars correspond to the total difference between the scratched area and the initial topographic image whereas the empty symbols correspond to the cumulate of differences between successive images. The colored area corresponds to the maximum error obtained with this last method. The insert shows an example of a 3D image after subtraction between two images.

204 resistance of materials. Considering the trace and retrace tip displacement
 205 over the abraded $1 \mu\text{m}^2$ square area, the volume V of removed polymer after
 206 N iterated abrasive scans may be expressed as

$$V = 2n_\ell N L A_T \quad (1)$$

207 where n_ℓ is the number of scan lines in the acquired topographic image (256
 208 scanning lines), N is the number of scans, L is the length of the abraded
 209 area ($1 \mu\text{m}$) and A_T is the projected frontal area in contact with the tip as
 210 schematized in Figure 2b. The validity of the above expression was checked
 211 on PMMA by measuring the removed volume as a function of n_ℓ , which was
 212 changed from 128 to 1024 scanning lines (data not shown). As expected for a
 213 linear scratching test, an increase of the removed volume was observed with
 214 the number of scanning lines. Therefore, the cohesive energy determined by
 215 [27] from the measured volume does not reflect only the intrinsic properties of
 216 the analysed material although the data may still be sufficient to determine
 217 mechanical properties such as the hardness.

218 The measurement of hardness requires the geometry of the indenter. The
 219 apex radius of the AFM tip was given by the manufacturer to be below 10
 220 nm but the tip wears off with calibration and reached a steady radius R value
 221 (see experimental section) that remains stable during probing process. With
 222 this spherical tip apex, the projected contact area A_N can be related to the
 223 frontal area A_T by the following relation:

$$A_N = \pi(2RA_T)^{2/3} \quad (2)$$

224 By definition, the hardness H of a material is the ratio between the
 225 applied normal force F_N and the area A_N under the tip (Figure 3b). Hence,
 226 we get the following relation between H and F_N :

$$F_N = H\pi(2RA_T)^{2/3} \quad (3)$$

227 The data points for A_T for different values of F_N are plotted for starch and
 228 gluten, as well as for PMMA, in Figure 5. The data are correctly fitted by
 229 Eq. (3) allowing for the determination of hardness H for each polymer (Table
 230 1).

231 The measured hardness of PMMA is consistent with previous data ob-
 232 tained with distinct approaches yielding a value between 0.3 GPa and 0.6
 233 GPa [31, 25, 32]. The hardness of gluten is found to be of the same order of

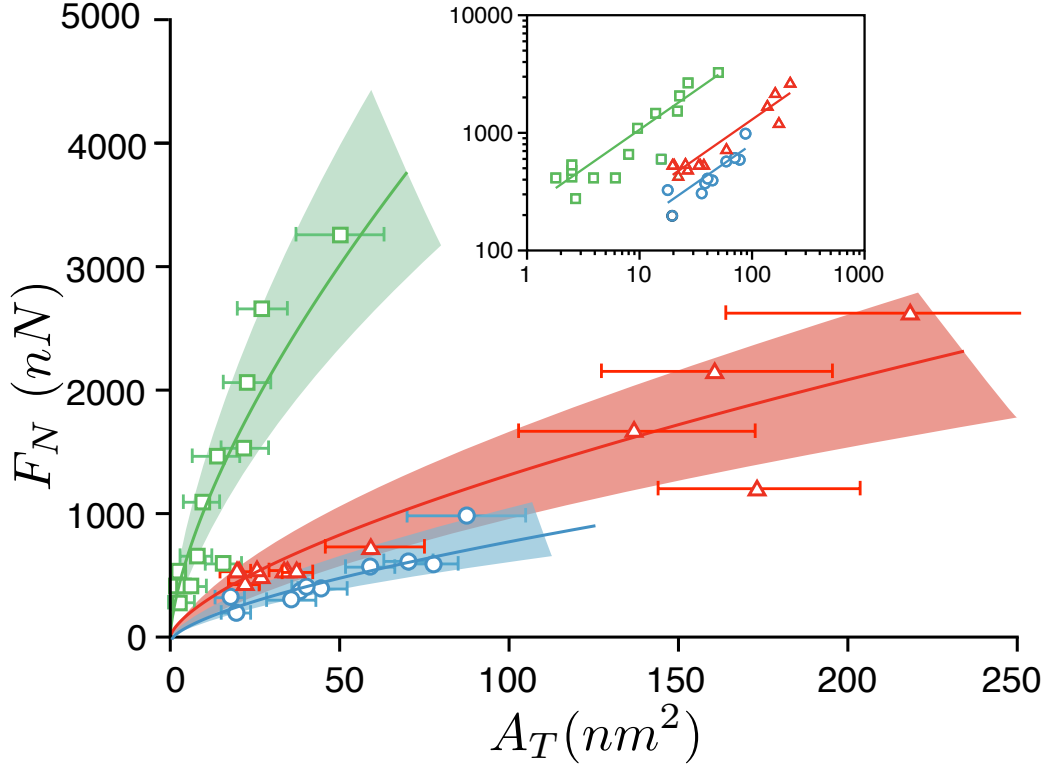


Figure 5: AFM data of the projected area A_T in front of the tip as a function of the normal force F_N for starch (green squares), gluten (red triangles) and PMMA (blue circles). Error bars on A_T represent measurement errors on the depth z and thus on the removed polymer volume V during abrasion. The full lines represent the predicted behavior by equation (3). The colored area around the fitting curve represents the error resulting from the tip radii variability. Insert: log-log representation of the same data.

234 magnitude as PMMA but four times lower than that of starch. The hardness
 235 of gluten at the nanoscale is thus close to that of soft materials, such as
 236 talc [35], and similar to other biopolymers such as wheat straw or other crop
 237 stalks [36], whereas the starch hardness is closer to that of calcite [35] and
 238 the values measured for core shells [37].

239 The observed hardness for starch and gluten is in a better agreement
 240 with the differences in the structure of the two biopolymers than earlier
 241 evaluations by micro-indentation [14, 15]. In fact, the gluten is characterized
 242 by a complex protein network [39] whereas the starch has a granular and
 243 semi-cristalline structure [43]. This discrepancy between our results at the
 244 nano-scale and those of earlier measurements by micro-indentation may be
 245 due to the scale of measurement or the orders of magnitude of the applied
 246 forces, as already pointed out in the literature [35, 24, 37]. In fact, a close look
 247 at the previous results obtained for wheat grains [15] or for purified starch
 248 and gluten dispersed in a polyester resin [14] indicate that the indentation
 249 depth was generally above 10 μm for applied forces of several mN. Therefore,
 250 at this resolution, the polymers in wheat grains are difficult to distinguish,
 251 and hence the measurement reflects in practice the hardness of the softer
 252 polymer. Furthermore, in Barlow et al. [14], the purified isolated polymers
 253 were included in a resin which was prone to modify the polymer properties.
 254 Indeed, the measured hardness of a single component in a composite material
 255 was found to be highly dependent on the dimensions of indenter [38].

Table 1: Hardness H and apparent friction coefficient μ_{app} obtained by AFM for gluten, starch and PMMA.

	H (MPa)	μ_{app}
Gluten	640 ± 170	0.39 ± 0.05
Starch	2400 ± 600	0.32 ± 0.05
PMMA	400 ± 100	0.59 ± 0.05

256 The mechanical properties of PMMA, as a bulk material, as obtained
 257 with AFM were also compared with the data obtained by indentation at the
 258 nanoscale. The nanoindentation assays confirmed the PMMA hardness even
 259 with a better accuracy at 420 ± 30 MPa, which is similar to those reported in
 260 previous studies [31, 32]. But gluten and starch, which respectively display a
 261 complex protein network and a granular structure [39, 3] were more difficult
 262 to explore. A number of indentation tests on these two polymers had to be
 263 discarded due to the sliding of the indenter during the assay. However, the

264 data obtained confirmed the difference between the two biopolymers with a
 265 hardness between 400 and 760 MPa for gluten and between 1000 and 2600
 266 MPa for starch. Nevertheless, we observed a higher variability of the mea-
 267 surements for this type of polymers in nanoindentation assays.

268 3.3. Shear strength determination

269 The friction coefficient μ_{app} at the interface between two solid bodies at
 270 the nanoscale can be evaluated from the friction force F_T , recorded during
 271 AFM nano-scratching test, and the applied normal force F_N [40, 25]:

$$\mu_{app} = \frac{F_T}{F_N} \quad (4)$$

272 Figure 6 shows the mean value of F_T versus F_N for each polymer. The data
 273 collapse on a straight line passing through the origin. The apparent friction
 274 coefficient μ_{app} is given by the slope and its values are presented in Table 1.
 275 The measured values of μ_{app} are quite close for starch and gluten and about
 276 1.5 to 2 times below that of PMMA².

277 It is worth noting that this apparent friction coefficient μ_{app} measured at
 278 the nanoscale can not be directly interpreted as Amonton's friction coefficient
 279 measured at the macroscopic scale, where multi-asperity contact is assumed
 280 [29]. In fact, in scratching of a soft material at the nanoscale, the apparent
 281 friction occurs at a single asperity from the addition of two effects:

- 282 • Interfacial shear in a small layer of the material;
- 283 • Visco-elastoplastic flow of material around the scratching tip.

284 In all models described in the literature, the interfacial shear was character-
 285 ized by adhesion or a real friction coefficient μ_{true} , which is of special interest
 286 as it is linked to the mechanical hardness through equation:

$$\mu_{true} = \frac{\tau}{H} \quad (5)$$

²The vanishing of the friction force with normal force means that F_N is the real contact reaction force including both the compressive force exerted vertically on the tip and the cohesive van der Waals force exerted by the surface on the AFM tip. This is because the reference state for the deflection of the cantilever is the force-free state, so that the deflection of the cantilever is the resultant of both the attraction force and compressive forces acting at the tip.

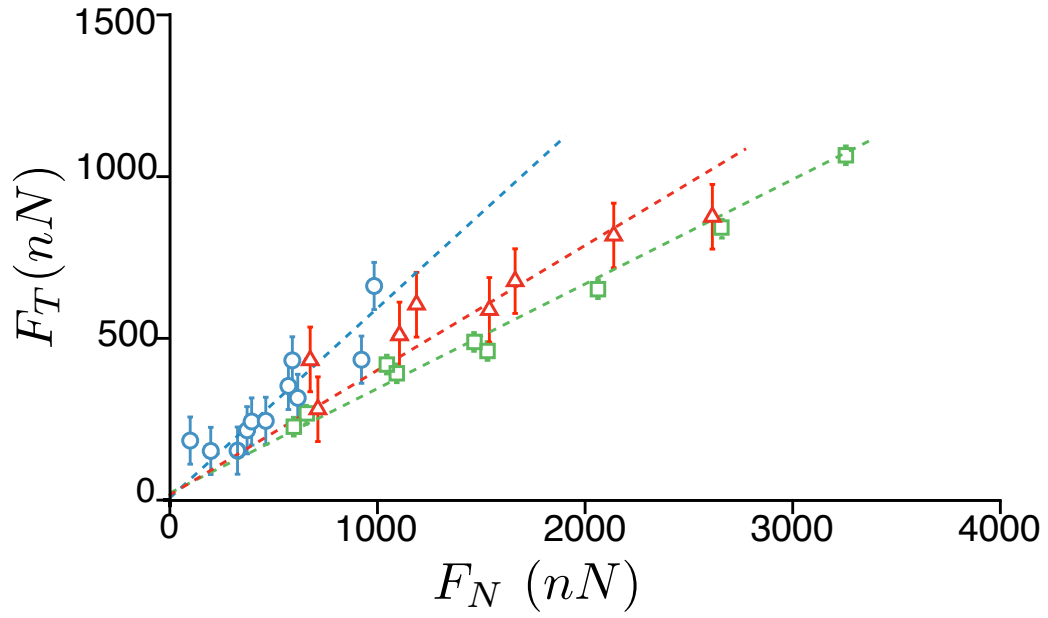


Figure 6: Friction force F_T plotted against normal force F_N for starch (green squares), gluten (red triangles) and PMMA (blue circles). The error bars represent the standard deviation of F_T for ten independent abrasive scans. The data are fitted by a straight line crossing the origin.

287 where τ is the shear strength of the material. The measured apparent co-
 288 efficient is thus comprised between the real friction coefficient and a higher
 289 value [41], which depends on the behavior of the scratched material under
 290 experimental conditions (applied forces, tip geometry, strain velocity, tem-
 291 perature).

292 If the polymers were totally elastic, we would have $\mu_{app} = \mu_{true}$ and the
 293 shear strength could be estimated by equation (5). In this case, the values
 294 of the shear strength τ for gluten, starch and PMMA would be equal to
 295 250 MPa, 768 MPa and 236 MPa, respectively. However, during the test,
 296 the polymers are not in the elastic domain because of scratching and plastic
 297 deformation leaving a track as observed in Figure 3, c-c'. Therefore, the
 298 apparent friction coefficient μ_{app} should be modified by subtracting the effect
 299 of the front created ahead of the moving tip with a ploughing coefficient
 300 μ_{plough} :

$$\mu_{true} = \mu_{app} - \mu_{plough} \quad (6)$$

301 The coefficient μ_{plough} may be evaluated from the rear contact angle ω in front
 302 of the tip along the scratching assay and the radius of contact determined
 303 by in-situ measurement on a homogeneous and transparent material [29].
 304 However, in our AFM conditions, the measurement of those parameters were
 305 not possible. But for PMMA it has a value between 0.1 and 0.2 according
 306 to previously reported data [41, 42]. Taking into account the ploughing
 307 correction, μ_{true} is found to be comprised between 0.39 and 0.49 ± 0.05 , and
 308 thus the shear strength τ is found to be between 156 ± 59 MPa and 196 ± 68
 309 MPa. These values of μ_{true} and τ are consistent with the previous scratching
 310 studies developed on PMMA using similar conditions of temperature, strain
 311 rate and contact pressure but different method of measurement [29].

312 Assuming that gluten and starch have a similar elasto-plastic behavior,
 313 we may use the same value of μ_{plough} in equation (6) to estimate μ_{true} for
 314 starch and gluten. The resulting shear strength is then comprised between
 315 122 ± 64 MPa and 185 ± 80 MPa for gluten, thus close to that of PMMA,
 316 and between 288 ± 192 MPa and 528 ± 248 MPa for starch. In all cases,
 317 starch shows two to three times more strength than gluten in scratching
 318 tests, supporting once more the difference in mechanical behavior of these
 319 two biopolymers as it was already discussed with hardness measurements.

320 4. Conclusions

321 In this paper, AFM scratching assays were performed with two important
322 biopolymers, starch and gluten. Our findings reveal a higher resistance to
323 fracture and a less friction coefficient for starch compared to gluten, the later
324 being closer to our reference material PMMA. These data will serve to refine
325 a numerical model of the starchy endosperm fractionation process. Given
326 the broad use of these two biopolymers in food and non-food products, the
327 described method also appears helpful in order to further explore the me-
328 chanical properties of starch and gluten in a wide range of conditions of tem-
329 perature, relative humidity and stresses. In contrast with nanoindentation,
330 this AFM scratching assay also allows to map the local mechanical properties
331 and assess the potential heterogeneity of the material at a nanoscale level.
332 This method thus appears an interesting alternative to characterize any type
333 of polymers. It also opens the way to determine the mechanical properties
334 of each of the components in a composite material and possibly the polymer
335 interface.

336 5. Acknowledgement

337 We would like to thank F. Baudoin (UMR IATE, Montpellier) for his kind
338 gift of wheat grain purified starch and gluten and S. Calas-Etienne (Univer-
339 sity Montpellier 2) for the nano-indentation assays. We are also grateful to
340 Montpellier 2 University and CEPIA department of INRA for the PhD grant
341 of E. Chichti.

- 342 [1] F. Xie, P. J. Halley, L. Averous, Rheology to understand and optimize
343 processibility, structures and properties of starch polymeric materials,
344 Prog. Polym. Sci. 37 (4) (2012) 595–623.
- 345 [2] D. Zaidel, N. Chin, Y. Yusof, A review on rheological properties and
346 measurements of dough and gluten, J. Applied Sci. 10 (20) (2010) 2478–
347 2490.
- 348 [3] H. Cornell, The functionality of wheat starch. In Starch in Food, Struc-
349 ture Function and Applications, Woodhead publishing Ld., Cambridge,
350 UK, 2004, pp. 211–240.
- 351 [4] T. Evers, S. Millar, Cereal grain structure and development: Some im-
352 plications for quality, J. Cereal. Sci. 36 (3) (2002) 261–284.

- 353 [5] L. Averous, Biodegradable multiphase systems based on plasticized
354 starch: A review, *J. Macromol. Sci.-Pol. R. C44* (3) (2004) 231–274.
355 doi:10.1081/mc-200029326.
- 356 [6] H. Zhang, G. Mittal, Biodegradable protein-based films from plant re-
357 sources: A review, *Environmental Progress and Sustainable Energy*
358 29 (2) (2010) 203–220. doi:10.1002/ep.10463.
- 359 [7] S. Guilbert, C. Guillaume, N. Gontard, *Food Engineering Series*,
360 Springer, 2011, pp. 619–630.
- 361 [8] C. Andersson, New ways to enhance the functionality of paperboard
362 by surface treatment - a review, *Packag. Technol. Sci.* 21 (6) (2008)
363 339–373. doi:10.1002/pts.823.
- 364 [9] J. Jane, C. Maningat, R. Wongsagonsup, Starch characterization, vari-
365 ety and application. In *Industrial crops and uses*, Singh, B. P., 2010, pp.
366 207–235.
- 367 [10] Z. Wang, Z. Li, Z. Gu, Y. Hong, L. Cheng, Preparation, characterization
368 and properties of starch-based wood adhesive, *Carbohydr. Polym.* 88 (2)
369 (2012) 699–706. doi:10.1016/j.carbpol.2012.01.023.
- 370 [11] S. Khosravi, P. Nordqvist, F. Khabbaz, M. Johansson, Protein-based ad-
371 hesives for particleboards-effect of application process, *Ind. Crop. Prod.*
372 34 (3) (2011) 1509–1515. doi:10.1016/j.indcrop.2011.05.009.
- 373 [12] V. Topin, J.-Y. Delenne, F. Radjai, L. Brendel, F. Mabilie, Strength and
374 failure of cemented granular matter, *Eur Phys J E Soft Matter* 23 (4)
375 (2007) 413–29. doi:10.1140/epje/i2007-10201-9.
- 376 [13] V. Topin, F. Radjai, J.-Y. Delenne, F. Mabilie, Mechanical modeling of
377 wheat hardness and fragmentation, *Powder Technol.* 190 (1-2) (2009)
378 215–220. doi:10.1016/j.powtec.2008.04.070.
- 379 [14] K. K. Barlow, M. S. Buttrose, D. H. Simmonds, M. Vesk, The nature
380 of the starch-protein interface in wheat endosperm, *Cereal Chem.* 50
381 (1973) 443–454.
- 382 [15] G. M. Glenn, R. K. Johnston, Mechanical-properties of starch, protein
383 and endosperm and their relationship to hardness in wheat, *Food Struct.*
384 11 (3) (1992) 187–199.

- 385 [16] G. Binnig, C. F. Quate, C. Gerber, Atomic force microscope, *Phys. Rev.*
386 *Lett.* 56 (9) (1986) 930–933. doi:10.1103/PhysRevLett.56.930.
- 387 [17] D. Fotiadis, S. Scheuring, S. A. Muller, A. Engel, D. J. Muller, Imaging
388 and manipulation of biological structures with the afm, *Micron* 33 (4)
389 (2002) 385–397. doi:10.1016/S0968-4328(01)00026-9.
- 390 [18] N. C. Santos, M. A. R. B. Castanho, An overview of the biophysical
391 applications of atomic force microscopy, *Biophys. Chem.* 107 (2) (2004)
392 133–149. doi:10.1016/j.bpc.2003.09.001.
- 393 [19] P. M. Baldwin, J. Adler, M. C. Davies, C. D. Melia, High resolution
394 imaging of starch granule surfaces by atomic force microscopy, *J. Cereal.*
395 *Sci.* 27 (3) (1998) 255–265. doi:10.1006/jcrs.1998.0189.
- 396 [20] S. Neethirajan, D. J. Thomson, D. S. Jayas, N. D. G. White, Character-
397 ization of the surface morphology of durum wheat starch granules using
398 atomic force microscopy, *Microsc. Res. Techniq.* 71 (2) (2008) 125–132.
399 doi:10.1002/jemt.20534.
- 400 [21] A. Paananen, K. Tappura, A. S. Tatham, R. Fido, P. R. Shewry,
401 M. Miles, T. J. McMaster, Nanomechanical force measurements
402 of gliadin protein interactions, *Biopolymers* 83 (6) (2006) 658–667.
403 doi:10.1002/bip.20603.
- 404 [22] A. D. L. Humphris, T. J. McMaster, M. J. Miles, S. M. Gilbert, P. R.
405 Shewry, A. S. Tatham, Atomic force microscopy (afm) study of inter-
406 actions of hmw subunits of wheat glutenin, *Cereal Chem.* 77 (2) (2000)
407 107–110. doi:10.1094/CCHEM.2000.77.2.107.
- 408 [23] L. Scudiero, C. F. Morris, Field emission scanning electron and
409 atomic force microscopy, and raman and x-ray photoelectron spec-
410 troscopy characterization of near-isogenic soft and hard wheat ker-
411 nels and corresponding flours, *J. Cereal Sci.* 52 (2) (2010) 136–142.
412 doi:10.1016/j.jcs.2010.04.005.
- 413 [24] B. Bhushan, X. D. Li, Nanomechanical characterisation of solid
414 surfaces and thin films, *Int. Mater. Rev.* 48 (3) (2003) 125–164.
415 doi:10.1179/095066003225010227.

- [25] S. E. Flores, M. G. Pontin, F. W. Zok, Scratching of elastic/plastic materials with hard spherical indenters, *J. Appl. Mech.-T. ASME* 75 (6) (2008) 061021. doi:10.1115/1.2966268.
- [26] N. E. Kurland, Z. Drira, V. K. Yadavalli, Measurement of nanomechanical properties of biomolecules using atomic force microscopy, *Micron* 43 (2-3) (2012) 116–128. doi:10.1016/j.micron.2011.07.017.
- [27] F. Ahimou, M. J. Semmens, P. Novak, G. Haugstad, Biofilm cohesive measurement using a novel atomic force microscopy methodology, *Applied Environ. Microbiol.* 73 (9) (2007) 2897–2904.
- [28] S. Lafaye, M. Troyon, On the friction behaviour in nanoscratch testing, *Wear* 261 (7-8) (2006) 905–913. doi:10.1016/j.wear.2006.01.036.
- [29] S. Lafaye, C. Gauthier, R. Schirrer, Analysis of the apparent friction of polymeric surfaces, *J. Mater. Sci.* 41 (19) (2006) 6441–6452. doi:10.1007/s10853-006-0710-7.
- [30] F. Auger, M.-H. Morel, M. Dewilde, A. Redl, Mixing history affects gluten protein recovery, purity, and glutenin re-assembly capacity from optimally developed flour-water batters, *J. Cereal Sci.* 49 (3) (2009) 405–412. doi:10.1016/j.jcs.2009.01.008.
- [31] A. Karimzadeh, M. R. Ayatollahi, Investigation of mechanical and tribological properties of bone cement by nano-indentation and nano-scratch experiments, *Polym. Test.* 31 (6) (2012) 828–833. doi:10.1016/j.polymertesting.2012.06.002.
- [32] G. H. Wei, B. Bhushan, N. Ferrell, D. Hansford, Microfabrication and nanomechanical characterization of polymer microelectromechanical system for biological applications, *J. Vac. Sci. Technol. A* 23 (4) (2005) 811–819. doi:10.1116/1.1861937.
- [33] J. L. Hutter, J. Bechhoefer, Calibration of atomic-force microscope tips (vol 64, pg 1868, 1993), *Rev. Sci. Instrum.* 64 (11) (1993) 3342–3342. doi:10.1063/1.1144449.
- [34] B. D. Morton, H. Wang, R. A. Fleming, M. Zou, Nanoscale surface engineering with deformation-resistant core-shell nanostructures, *Tribol. Lett.* 42 (1) (2011) 51–58. doi:10.1007/s11249-011-9747-0.

- 448 [35] J. A. Williams, Analytical models of scratch harness, *Tribology Int.* 29
449 (1996) 675–694.
- 450 [36] Y. Wu, S. Wang, D. Zhou, C. Xing, Y. Zhang, Z. Cai, Evalua-
451 tion of elastic modulus and hardness of crop stalks cell walls by
452 nano-indentation, *Bioresource Technol.* 101 (8) (2010) 2867–2871.
453 doi:10.1016/j.biortech.2009.10.074.
- 454 [37] T. Shean, M. Oyen, M. Ashby, *Handbook of nanoindentation with bio-*
455 *logical applications*, Pan Stanford Pub., Singapore, 2011, pp. 1–22.
- 456 [38] C. Scheuerlein, T. Boutboul, D. Leroy, L. Oberli, B. Rehmer, Hardness
457 and tensile strength of multifilamentary metal-matrix composite super-
458 conductors for the large hadron collider (lhc), *J. Mater. Sci.* 42 (12)
459 (2007) 4298–4307. doi:10.1007/s10853-006-0633-3.
- 460 [39] V. Kontogiorgos, Microstructure of hydrated gluten network, *Food. Res.*
461 *Int.* 44 (9) (2011) 2582–2586. doi:10.1016/j.foodres.2011.06.021.
- 462 [40] F. Bowden, D. Tabor, *The friction and lubrication of solids*, Oxford
463 University Press, London, 1951.
- 464 [41] S. Lafaye, C. Gauthier, R. Schirrer, A surface flow line model of a
465 scratching tip: apparent and true local friction coefficients, *Tribol. Int.*
466 38 (2) (2005) 113–127. doi:10.1016/j.triboint.2004.06.006.
- 467 [42] S. Lafaye, C. Gauthier, R. Schirrer, The ploughing friction: analytical
468 model with elastic recovery for a conical tip with a blunted spherical
469 extremity, *Tribol. Lett.* 21 (2) (2006) 95–99. doi:10.1007/s11249-006-
470 9018-7.
- 471 [43] A. Buleon, P. Colonna, V. Olanchot, Starch granules: structure and
472 biosynthesis, *Int. J. Biol. Macromol.* 23 (1998) 85–112.